An entropy based feature extraction and classification of vibroarthographic signal using improved complete ensemble empirical mode decomposition with adaptive noise

Article *in* IET Science Measurement ? Technology · December 2017

DOI: 10.1049/iet-smt.2017.0284

CITATIONS
14

READS
829

3 authors:

Saif Nalband
DY Patil International University
10 PUBLICATIONS **79** CITATIONS
SEE PROFILE

A Amalin Prince
BITS Pilani, K K Birla Goa
34 PUBLICATIONS **142** CITATIONS
SEE PROFILE

Anita Agrawal
BITS Pilani, K K Birla Goa
24 PUBLICATIONS **134** CITATIONS
SEE PROFILE

IET Science, Measurement & Technology

Research Article

IET Journals
The Institution of Engineering and Technology

Entropy-based feature extraction and classification of vibroarthographic signal using complete ensemble empirical mode decomposition with adaptive noise

ISSN 1751-8822
Received on 28th June 2017
Revised 7th October 2017
Accepted on 10th December 2017
E-First on 16th January 2018
doi: 10.1049/iet-smt.2017.0284
www.ietdl.org

Saif Nalband[1], Amalin Prince[1] ✉, Anita Agrawal[1]

[1]*Department of Electrical and Electronics Engineering, Birla Institute of Technology and Science, Pilani, KK Birla, Goa Campus, Goa 403726, India*

✉ *E-mail: amalinprince@gmail.com*

Abstract: Non-invasive methods accomplished by a computer aided diagnosis of knee-joint disorders provide an effective tool. The objective of this study is to analyse vibroarthographic (VAG) signals using non-linear signal processing technique. This study includes different entropy-based feature extraction techniques to attain highly distinguishable features. The authors proposed to use a non-linear method known as complete ensemble empirical mode decomposition with adaptive white noise to decompose the VAG signals into intrinsic mode functions (IMFs). Entropy-based features involving approximate entropy, sample entropy, Shannon entropy, Rényi entropy, Tsallis entropy and permutation entropy (PeEn) are computed from dominant IMFs and reconstructed VAG signals. These extracted features are given as input to the least squares support vector machine as a classifier. The results illustrated that PeEn performed better with respect to other entropies. PeEn gives a classification accuracy of 86.61% and Matthews correlation coefficient of 0.7082. The computational complexity of entropies was also analysed. Results inferred that PeEn has a computational complexity of $O(N)$ provided a simple, robust and low computational feature extraction technique. Analysis of VAG signals using non-linear preprocessing and entropy-based features can provide highly distinguishable features for accurate detection of knee-joint disorders.

1 Introduction

The knee-joint is one of the most vulnerable parts of the human body. It can resist a significant amount of stress and strain while engaging in routine life activities or sports activities [1]. As a result, the knee-joints are quite susceptible to various injury risks. These injuries are induced by degradation of articular cartilage (wear and tear of muscles/tissues). Thus, interpreting the deterioration of the knee-joint should be probed in earlier stages. Procedures based on invasive and non-invasive medical techniques are available for the diagnosis [2]. Arthroscopy, an example of invasive technique and non-invasive techniques such as X-rays, magnetic resonance imaging and so on are some of the popular procedures available in assessing knee-joint disorders. However, these procedures fail to provide the dynamic assessment of knee-joint disorders. Cost and limitation in routine checkups are other major concern about these procedures. Considering these drawbacks, an alternative non-invasive and low cost knee-joint diagnosis is explored using vibroarthographic (VAG) signals [3]. The VAG is the vibration or the audio signals emitted from the patellafemoral joint during the active knee-joint movements. These signals contain information that could characterise a pathological aspect of the knee-joint disorders. These signals are non-linear and non-stationary by nature. Hence, the assessment of knee-joint disorders with VAG signals using digital signal processing techniques offers a safe, low-cost and non-invasive clinical tool for the early detection knee-joint disorder.

The characteristics obtained from VAG signals could be utilised in discriminating and detecting abnormalities in VAG signals. Researchers have successfully carried out the analysis of VAG signals by various feature extraction methodologies. These extracted features are significant as they are correlated with the degraded articular cartilage. The research group of Rangayyan *et al.* [4–7] has worked extensively in various feature extraction algorithms. Shark *et al.* [8, 9] have used the knee acoustic emission biomarkers for the assignment of knee-joint related to ageing and degeneration. Baczkowicz *et al.* [10–12] have carried out the analysis of VAG signal with respect to age specific and vibration signal generated from different levels of cartilage destruction. Wu *et al.* have carried out features extraction by the representation of fluctuation using kernel density modelling method of VAG signals [13]. Another major contribution in the analysis of the VAG signals has been covered in review paper and book by Wu *et al.* [14, 15]. Nalband *et al.* [16] have carried out the analysis of VAG signal using wavelet decomposition-based feature extraction. The VAG signals were decomposed into sub-band signals by wavelet decomposition. However, these sub-band signals were still contaminated with artefacts. These artefacts included external noise, muscle contraction interference, baseline wanders and so on. These artefacts could cause some serious effects in inferring the results. The previous study on VAG signals has been carried out by assuming linearity nature of VAG signals and thereby utilising linear methodologies. Since VAG signals are non-linear and non-stationary in nature, non-linear signal processing techniques have been explored in this work. The literature survey also revealed that non-linear techniques accomplished by feature extraction techniques could improve in discriminating between healthy and abnormal VAG signals. This improvement would be in building an effective classification model.

Huang *et al.* [17] proposed a non-linear and non-stationary signal processing technique known as the empirical mode decomposition (EMD). Wu *et al.* [18] applied EMD for the analysis of VAG signal for detecting chondromalacia patellae. Chen *et al.* [19] applied Hilbert–Huang transform (HHT) for the analysis of VAG signals. EMD has been used for the analysis of biomedical signals [20]. However, EMD has one major disadvantage of mode mixing. In mode mixing, a particular intrinsic mode function (IMF) is composed of signals with widely disparate scales, or a signal identical scale may reside in different IMF components. To overcome this problem ensemble EMD (EEMD) was proposed [21]. Wu *et al.* [22] applied EEMD for the analysis of VAG signal. EEMD has been studied as an improved preprocessing technique for VAG signals. EEMD overcomes the problem of mode mixing by adding white noise along with the original signal. EMD is performed on the original signal but the

true IMFs are obtained through an ensemble mean. Wu *et al.* [23] further analysed VAG signals using EEMD and extracting three entropies and three distinct envelope amplitude parameters as features. Nalband *et al.* [24] have used EEMD and three entropy based features such as Tsallis entropy (TsEn), permutation entropy (PeEn) and spectral entropy. Their performance was evaluated using the random forest as a classifier.

This work proposes to use complete EEMD with adaptive noise (CEEMDAN) for the analysis of VAG signal [25]. CEEMDAN provides an improvement in minimising the reconstructed error, providing a fixed number of modes for different signals and minimises residual noise present in the mode [25]. CEEMDAN has been successfully reported in the analysis of non-stationary [26] and non-linear data, especially in cases of biomedical signals [25]. Hence, we explore CEEMDAN as a preprocessing technique in this work. Entropy, which is a quantified measure of the complexity of the signals, is investigated. Approximate entropy (ApEn), sample entropy (SampEn), Shannon entropy (ShEn), Rényi entropy (ReEn), TsEn and PeEn as entropy-based feature extraction techniques have been proposed in this investigation. Furthermore, the EMD along with entropy based features has been applied for various applications related to biomedical image processing [27, 28]. Reported literature revealed that entropy-based features have been extensively studied in the analysis of biomedical signals [29–32]. In the proposed work, the VAG signals are decomposed into IMFs by CEEMDAN. The VAG signals are reconstructed by dominant IMFs of VAG signals. Entropy-based features are extracted from the dominant IMFs and from the reconstructed VAG signals. Finally, the obtained extracted features are given to classifier in order to analyse their performance. Least squares support vector machine (LS-SVM) as a classifier is proposed in this study. Moreover, we have computed and compared the computational complexity of feature extraction techniques. Hence, the computational complexity of the entire proposed system has been computed. The proposed methodology could provide an aid in developing a non-invasive and low-cost diagnostic system for knee-joint disorders. Such methods would enhance the rehabilitation program by monitoring knee-joints disorders in a cost effective manner.

The remaining of this paper is organised as follows: Section 2 presents the CEEMDAN method, features extraction techniques of entropies and the classification techniques. The VAG dataset and experimental results have been provided in Section 3 and the discussion has been presented in Section 4. Finally, Section 5 would conclude the paper.

2 Methodology

2.1 Complete EEMD with adaptive noise

EMD is a data-dependent approach suitable for decomposition of a non-linear and non-stationary signal into symmetric, amplitude and frequency modulated components known as intrinsic mode functions (IMFs) [17]. IMFs of the signal are considered when following of two conditions are fulfilled: (a) the number of maxima/minima (extrema) and the number of zero crossing should be equal or differ by one (b) the mean of upper and lower envelopes (local mean) must be zero. In the case of EEMD, the IMFs are computed as the mean of the corresponding IMFs obtained from an ensemble of the original signal with additional of finite variance white noise [21]. The EEMD overcomes the problem of mode mixing as EEMD is a multiple trial process and each trial has the similar procedure as EMD, except that the input signal is a mixture of the original signal and a finite Gaussian white noise [21]. The scale separation capabilities of EEMD enable to eliminate the problem of mode mixing. However, there are some disadvantages of EEMD and they are as follows: (i) the decomposition of the signal is usually incomplete and residual noise are attached in the modes, (ii) different modes are produced by the addition of noise with the signal. The number of sifting processes increases with the increase in the number of trials [25]. In order to overcome these disadvantages, CEEMDAN has been reported.

The steps for CEEMDAN are as follows: Let $M(.)$ be the operator producing local means of the signal. $E_k(.)$ be the operator producing $k_{(th)}$ mode obtained by the EMD. And let $w^{(i)}$ be the white Gaussian noise added having zero mean and variance as 1.

(1) The first residue is computed from local means of I realisation $x^{(i)} = x + \beta E_1(w^{(i)})$ by EMD

$$r_1 = \left\langle M(x^{(i)}) \right\rangle \tag{1}$$

(2) The first mode is calculated for $k = 1$

$$d_1 = x - r_1 \tag{2}$$

(3) The second residue is computed as the average of local means $r_1 + \beta E_2(w^{(i)})$ and the second mode is computed as

$$d_2 = r_1 - r_2 = r_1 - \left\langle M(r_1 + \beta_1 E_2(w^{(i)})) \right\rangle \tag{3}$$

(4) The K_{th} residue is calculated as

$$\left\langle M(r_{k-1} + \beta_{k-1} E_k(w^{(i)})) \right\rangle \tag{4}$$

(5) k_{th} mode is evaluated as

$$d_k = r_{k-1} - r_k \tag{5}$$

(6) Repeat from step 4 for next k.

The CEEMDAN algorithm's parameter are optimised by setting the amplitude of added Gaussian noise and complete ensemble number by statistical rule suggested by Wu and Huang [21]

$$\beta_n = \frac{\beta}{\sqrt{NE}} \tag{6}$$

Here NE is the ensemble number, β is the added Gaussian noise and β_n is the SD (standard deviation) of error which is the difference between the input data and its IMFs. The stopping criteria can be set either by means of energy parameter or by fixing the shifting iteration. Hence, in this study, the following parameters were set as follows:

(a) The complete ensemble number was set as $NE = 100$. This was the mean of IMFs obtained from 100 trails of CEEMDAN.
(b) 0.2 times the SD of raw VAG signal was fixed as added Gaussian noise.
(c) The maximum number of shifting iteration NS was set to 5000.

2.2 Feature extraction

2.2.1 Approximate entropy: ApEn was introduced by Pincus [33] as a statistical measure of the stochastic, dynamic and deterministic system. The details regarding the computation of ApEn have been given in Pincus [33]. This methodology could help in differentiating the dynamic state between healthy and abnormal VAG signals. ApEn has successfully applied to analysis pathological data, such as computing heart rates from ECG [34]. Let N be the data length of the given time series data $t(n) = t(1)$, at (2), …, $t(N)$. For computing ApEn, tolerance window u and embedding dimension v are input parameters. Considering for a constant length of data points N, ApEn is computed as

$$\mathrm{ApEn}(v, u, N) = [C^v(u) - C^{v+1}(u)] \tag{7}$$

Here $C^v(u)$ infers the pattern of mean length v and $C^{v+1}(u)$ infers the pattern of mean length $v + 1$. Hence, the reported computational complexity for ApEn is $O(N^2)$ and was computed by Manis [35].

2.2.2 Sample entropy: Though ApEn was quite popular in computing for the stochastic, dynamic and deterministic system, there were some disadvantages. These disadvantages include relative dissimilarity, depending on the given length and biasing. ApEn was modified to overcome these disadvantages and Richman and Moorman [36] introduced SampEn. SampEn is relatively easy

to compute with respect to ApEn as it is independent of the time series data. Sampan is embedding entropy, which provides information about how the VAG signal fluctuates with time by comparing the time series with a delayed version of itself. SampEn has been explored in the area of biomedical signals, especially in the cases of EEG and VAG signals [16, 37, 38]. Let B be the total number of template matches of length v and A be the total number of forward matches of length $v+1$, SampEn is given as

$$\text{SampEn}(v, u, N) = -\ln\frac{A^v(u)}{B^v(u+1)} \tag{8}$$

The value for selecting v and u are quite critical in computing ApEn and SampEn. Pincus suggested that usually, the values for $v = 2$ and u ranging from 0.1 to 0.2 standard deviation of data provided significant statistically validity of ApEn [34, 39]. In the current investigation the values for embedding dimension v is set to 1 or 2, and tolerance window u is fixed in the range from 0.1 and 0.25 times the SD of the original time series. In this work, the value of v has been set to 2 and u is fixed to 20% of the SD of the data points. And N is data set points of the VAG signal($N = 8000$). The computational complexity of SampEn is $O(N^{3/2})$ given by Pan *et al.* [40].

2.2.3 Shannon entropy: The complexity of measurement series data or measure of information contend is carried out by ShEn [41]. Shannon proposed ShEn as a measure of the information, content or complexity of data. Shannon has proposed ShEn for use in communication domain. With greater entropy often associated with more randomness and less system order. In this work, ShEn is computed using power spectrum density (PSD) of the VAG signal in order to evaluate the dynamic complexity of the VAG signals. Steps involved in the computing ShEn are as follows:

(1) The spectrum of the signal is computed by applying Fourier transform (fast Fourier transform – FFT).
(2) The power spectrum is obtained by computing multiplication on itself of Fourier's transform of the signal. E_r denotes the power level of the frequency component.
(3) Probability density function is obtained by normalising the computed PSD

$$e_f = \frac{E_f}{\sum E_r} \tag{9}$$

(4) The ShEn is given as

$$\text{ShEn} = \sum_f e_f \log\left(\frac{1}{e_f}\right) \tag{10}$$

For calculating ShEn, FFT has to be computed. Since the computational complexity of FFT is $O(N\log(N))$, therefore the computational complexity of ShEn is approximately $O(N\log(N))$.

2.2.4 Rényi entropy: Rényi [42] introduced ReEn a mathematical generalisation of ShEn. Rényi defines the information measure in more general terms that would preserve additivity individual events. The ReEn in VAG signal represents the statistics as indices of diversity. The spikes or the high peaks of occurrence in abnormal VAG signals would be inferred as these events. The ReEn can be defined as

$$\text{ReEn}(\alpha) = \frac{1}{1-\alpha}\left(\sum_f e_f^{\alpha}\right), \quad \alpha > 0, \alpha \neq 1 \tag{11}$$

where α is the enabling measurement of uncertainty among the distribution and due to which ReEn is much more flexible. In our study, the value of α is taken as 2. Steps involved in ReEn are quite similar to computing ShEn. Since FFT is involved in the computation, ReEn also has the time complexity of $O(N\log(N))$.

2.2.5 Tsallis entropy: TsEn was presented by Constantino Tsallis is a generalisation of the standard Boltzmann–Gibbs entropy [43]. Tellenbach *et al.* proved that TsEn is also known as non-additive entropy is useful for characterising measures with non-Gaussian trends. TsEn is used for the analysis of VAG signals since VAG signals are characterised by multicomponent signals and non-Gaussian trends. TsENs are useful in the analysis since TsEn provides strong correlations between the different micro states in a system. TsEn can signify the complexity of the VAG signal. TsEn characterises the behaviour emulated by the VAG signals in spikes and bursts. The uncertainties could be modelled by the empirical value b. TsEn defined as follows:

$$\text{TsEn} = \frac{1 - \sum_{i=1}^{W} a_j^b}{b-1} \tag{12}$$

The parameter b is called as a non-extensively index, a_j is the probability of the jth state and $b \neq 1$. Since the VAG signals are non-stationary and non-linear, therefore it would be reasonable to consider VAG signals as a sub-extensive system (i.e. $b > 1$). In this work, $b = 2$ has been set for conducting simulations. The computational complexity of TsEn is $O(N\log(N))$ since it involves the similar steps of ShEn.

2.2.6 Permutation entropy: Bandt and Pompe [44] proposed low computation entropy to compute the irregularity and complexity of non-stationary and non-linear time series data as PeEn. It also has the advantage of being robust and computationally simple. For a given time series data of length N. The steps involved in computing PeEn are as follows:

Step 1: For computing, PeEn depends upon embedding dimension m which determines the amount of information is contained in each vector and the time delay t_d. The possibility of a maximum number of symbols is based on the value of m.
Step 2: The permutation of embedded dimension m gives the possible number of symbols. An embedded vector is formed and sorted in increasing order.
Step 3: The probability of each possible symbols are evaluated is given by

$$P_k = \frac{p_k}{L - m + 1} \tag{13}$$

where p_k is the number of instances of the k_th symbol of the data length L.
Step 4: PeEn for a non-linear and non-stationary time series data N can be computed as in terms of P_K as follows:

$$\text{PeEn} = -\sum_{1}^{k} P_k \log(P_k) \tag{14}$$

Banddt and Pompe suggested values of $m = 3, 4, 5, \ldots, 7$ and yet the values $m = 3$ or 4 might still be small. In this work, the values of m and t_d are 3 and 1, respectively, as most suitable values since various analysis of biomedical signals have been carried out [45, 46]. Considering the steps involved in the computation of PeEn, the computational complexity of PeEn is $O(N)$.

2.3 Classification

2.3.1 Least squares support vector machine (SVM): SVM is a machine learning algorithm used to discriminate binary data by formally defining a separating plane. It's a statistical learning of Vapnik–Chervonenkis dimension theory [47]. SVM has a small drawback, which is singled out by LS-SVM. While SVM solves convex for programming problems which involve very high computational load to program the function for optimisation, LS-SVM uses only linear equations [48]. The solutions obtained by SVM are extracted by batch algorithms whereas LS-SVM uses on-line adaptive algorithms to find the solution. Hence, it can be seen

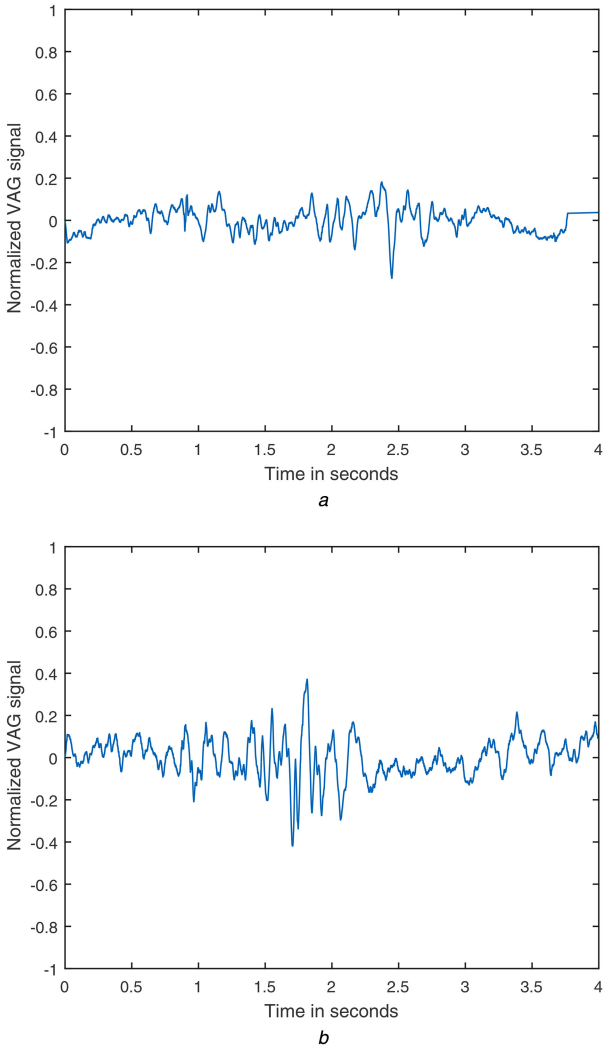

Fig. 1 *VAG signal of*
(a) Healthy and ***(b)*** Abnormal persons

that LS-SVM is simpler and hence widely used in various research areas, adaptive signal research being one of them. In our study, radial basis function as kernel function was used for LS-SVM. The effectiveness of the classifier can be evaluated using different performance parameters [20]. These parameters are as follows: (i) Matthews correlation coefficient (MCC), (ii) false discovery detection rate (FDR), (iii) sensitivity (SEN), (iv) specificity (SPF), (v) negative predictive value (NPV), (vi) positive predictive value (PPV) and (vii) accuracy (ACC).

3 Experiments

3.1 Dataset

Rangayyan and Wu [4, 5] carried out the data acquisition of knee-joint disorder at the University of Calgary, Canada. The ethical clearance for the experiment set was given by Conjoint Health Research Ethics Board of the University of Calgary. The experiment involved a total of 89 subjects and these subjects were examined by the physician. Among these 89 subjects, 51 (22 male, 29 female, age 28 ± 9.5 years) were considered as healthy since they did not suffer from any abnormalities of knee-joint pains or disorders. Thirty eight subjects (20 male, 18 female, age 35 ± 13.8 years) suffered from the various knee-joint disorders such as tibial chondromalacia, anterior cruciate ligament, meniscal tear and so on as reported by the physician. Each of these 89 subjects underwent a similar protocol of the experiment. The subjects were seated on a table in a relaxed mode. The position of the subject was fixed in such a manner that leg movements could be performed without any discomfort. At the mid-patella, a miniature accelerometer sensor was placed to acquire a signal from the knee-joint. The subject was instructed to flex and extend the legs in a period of 4 s. The electric voltage generated by the sensor is acquired in terms of acceleration and deceleration due to the knee-joint movements of the leg. National Instrument's LabView software and data acquisition board were used for amplifying and digitising the acquired VAG signal. The VAG signal was prefiltered (10Hz–1 kHz) and amplified. 2 kHz was the sampling frequency of the VAG signal and it was digitised having a 12-bit resolution [4]. A double cascaded moving average filter was applied to remove the baseline wander in the raw VAG signals [49]. An example of the filtered VAG signal can be seen in Fig. 1. Figs. 1*a* and *b* show the VAG signals of healthy and abnormal subjects, respectively.

3.2 Results

This study comprising of preprocessing (CEEMDAN), feature extraction techniques and classification technique has been implemented in MATLAB 2014a. The CEEMDAN decomposes VAG signals into a set of IMFs. From Fig. 2, it can be observed that different IMFs reveal different degrees of dynamics involved in the VAG signal. Figs. 2*a* and *b* show the IMFs obtained from the VAG signal for the healthy and abnormal subjects, respectively. IMF1–IMF3 represent the high-frequency oscillations, while IMF4–IMF12 represent the low-frequency oscillations. The high frequency IMF1 and IMF2 have flat envelopes and thereby do not represent pathological conditions of knee-joint disorders [22].

The detrended fluctuation analysis (DFA) algorithm is computed in order to analyse the correlation properties of each decomposed IMFs [22]. IMFs which contain the prominent information are identified based on the computed fractal scaling index. As suggested by Wu *et al.* [22], the IMFs have anti-correlation ($0 < \alpha < 0.5$) and baseline wander related IMFs (IMF9–IMF12) have been ignored. Hence, IMF5–IMF7 are considered as dominant data of the VAG signal. The obtained α values for IMF5–IMF7 are 1.302, 1.622 and 1.88, respectively. The VAG signals are reconstructed from the summation of these IMFs. Figs. 3*a* and *b* show the reconstructed VAG signals for healthy and abnormal subjects, respectively.

3.3 Feature extraction

After reconstructing the VAG signal, features were extracted from reconstructed VAG signals and from dominant IMFs (5–7). These features were extracted from 38 abnormal and 51 healthy VAG signals. Table 1 shows the mean and SD of entropy-based features of reconstructed VAG. Similarly, Tables 2 and 3 show the mean and SD of the IMFs (5–7) for healthy and abnormal VAG signals, respectively. From Tables 1–3, it can be observed that entropy-based features are high for abnormal VAG signals with respect to healthy VAG signals. The huge variability observed in features extracted from abnormal VAG signals is due to the presence of the high irregular vibrational components.

Kruskal–Wallis test was performed on the extracted features in order to infer the discrimination between the two distribution classes. Table 4 gives the *p*-value computed for extracted features from individual IMFs and reconstructed VAG signals. The table inferred that there is significant discrimination in the distribution of healthy and abnormal classes.

Boxplots of extracted features from the reconstructed VAG signals have been presented in Figs. 4 and 5. As observed from Figs. 4 and 5, abnormal distributions of extracted features show large variation with respect to the class of healthy VAG signals. Thus, the results obtained from the above statistics provided a significant distinction between healthy and abnormal VAG signals. Considering these results, the extracted features are given as inputs in building an effective classification model.

3.4 Classification

In this work, LS-SVM has used for classification of VAG signals. LS-SVM toolbox by De Brabanter *et al.* [50] has been used for implementing LS-SVM. Six entropy-based features were extracted from the reconstructed VAG signal and from dominant IMFs. The dataset consisted of 89 VAG samples. Training set has been set to

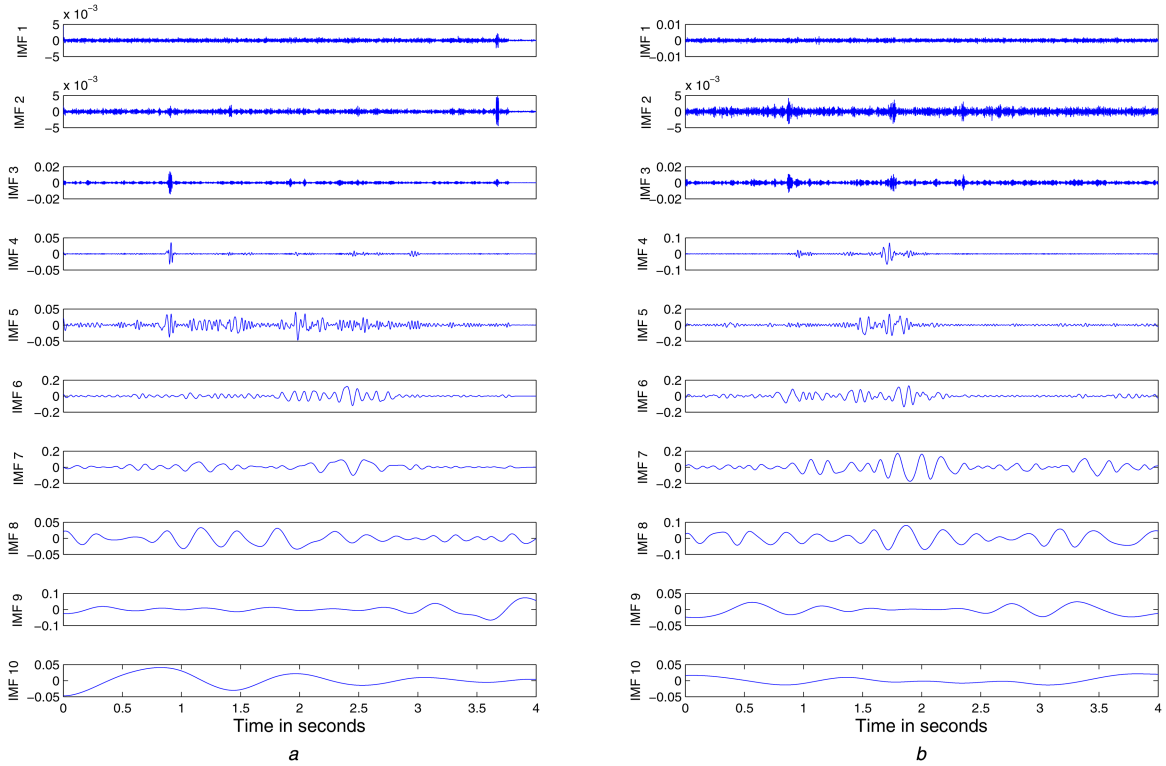

Fig. 2 *IMFs obtained from VAG signal of*
(a) Healthy and ***(b)*** Abnormal persons

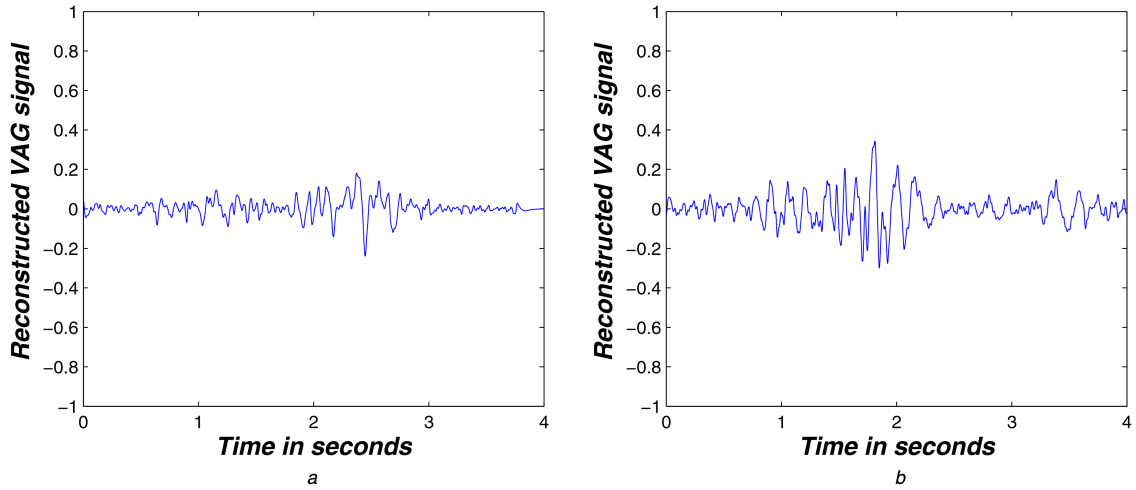

Fig. 3 *Reconstructed VAG signal of*
(a) Healthy and ***(b)*** Abnormal persons

Table 1 Statistical measures of features extracted from reconstructed VAG signals

Features	Mean ± standard deviation	
	Healthy	Abnormal
ApEn	0.000178 ± 0.00019	0.000301 ± 0.00023
SampEn	0.000182 ± 0.000201	0.000299 ± 0.000221
ShEn	0.239857 ± 0.165505	0.321193 ± 0.161272
ReEn	0.053276 ± 0.041809	0.073854 ± 0.041279
TsEn	0.051084 ± 0.038967	0.070421 ± 0.038454
PeEn	0.88832 ± 0.03444	0.967527 ± 0.024158

60% of healthy and abnormal VAG signals and remaining signals were considered as a test set. Targets belonging to abnormal VAG signals are chosen as 1 and healthy signals are set to 0. A tenfold cross-validation procedure has been used in order to assess the classification performance of the classifier [51]. The classification of individual features and vector of features considered in this study underwent a tenfold cross-validation. Radial basis function (RBF) has been used as a kernel function for the LS-SVM classifier. Command '(tunelssvm)' from LS-SVMlab Toolbox was used to determine the tuning parameters (e.g. the regularisation and kernel parameters) of the LS-SVM. The tuning parameters of LS-SVM are a two-step procedure. Initially, coupled simulated annealing algorithm is used for determining the parameters of LS-SVM. In the next step, the parameters are given to simplex or gridsearch algorithm for determining the optimised regularisation constant and kernel parameters. In our study, the classification results were found to be more effective using a gridsearch algorithm. The classification has been carried out for 200 iterations and the best classification results were stored. The performance of the classifier was hugely based on area under the receiver operating curve (ROC-AUC), SEN, SPF and ACC. Other parameters such as PPV, NPV, MCC and FDR were also considered for the evaluation purpose.

The performance of classification was analysed from the features extracted from reconstructed VAG signals and dominant

Table 2 Statistical measures of healthy IMFs for various entropy-based features

Features	Mean ± standard deviation		
	IMF 5	IMF 6	IMF 7
ApEn	0.000296 ± 0.000862	0.001545 ± 0.000669	0.000732 ± 0.000384
SampEn	0.000206 ± 0.000192	0.000327 ± 0.000268	0.000395 ± 0.000359
ShEn	0.221 ± 0.13924	0.31828 ± 0.15914	0.411 ± 0.22619
ReEn	0.0461 ± 0.03404	0.07411 ± 0.04335	0.10901 ± 0.07194
TsEn	0.040226 ± 0.02267	0.076586 ± 0.042422	0.113771 ± 0.069396
PeEn	0.91755 ± 0.02090	0.90685 ± 0.02075	0.80523 ± 0.01144

Table 3 Statistical measures of abnormal's IMFs for various entropy-based features

Features	Mean ± standard deviation		
	IMF 5	IMF 6	IMF 7
ApEn	0.000291 ± 0.000145	0.00018 ± 0.000122	0.000102 ± 0.000748
SampEn	0.000289 ± 0.000198	0.000412 ± 0.000309	0.000469 ± 0.00037
ShEn	0.250224 ± 0.11497	0.387123 ± 0.1568	0.506539 ± 0.218183
ReEn	0.052712 ± 0.028573	0.094697 ± 0.044253	0.140687 ± 0.071028
TsEn	0.050973 ± 0.026776	0.089486 ± 0.040154	0.129101 ± 0.061943
PeEn	0.93462 ± 0.02141	0.91465 ± 0.01962	0.81282 ± 0.01363

Table 4 *p*-Value for IMFs and reconstructed VAG signal

Features	IMF5	IMF6	IMF7	Recon
ApEn	0.512797	0.867984	0.208741	0.012657
SampEn	0.047229	0.197676	0.298865	0.014217
ShEn	0.1802	0.05728	0.05728	0.00969
ReEn	0.194909	0.0332	0.04386	0.00297
TsEn	0.121642	0.14583	0.294059	0.015059
PeEn	0.00025	0.20132	0.00998	0.000429

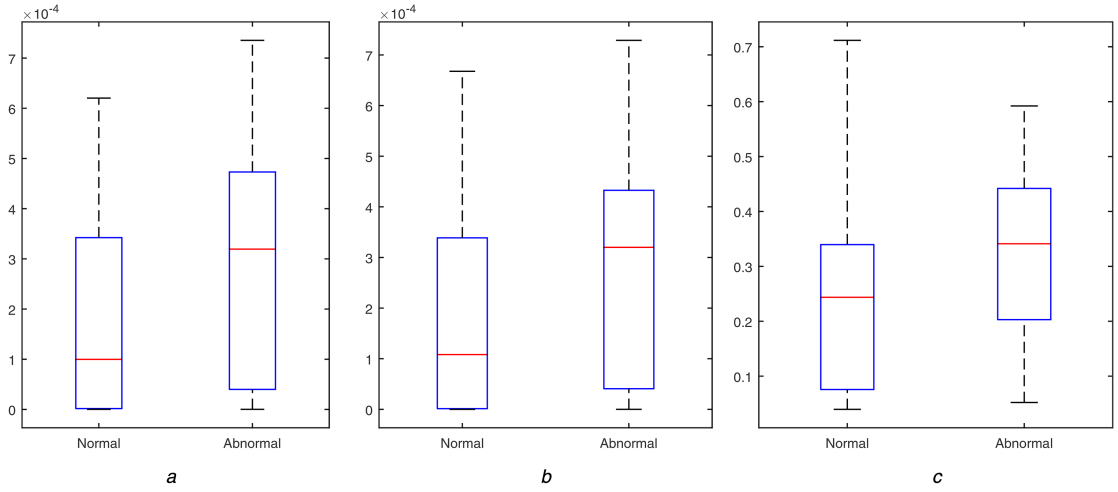

Fig. 4 *Boxplots of VAG signal of both healthy and abnormal persons*
(a) ApEn, ***(b)*** SampEn, ***(c)*** ShEn

IMFs (5–7). Table 5 gives the classification performance of VAG signal reconstructed from dominant IMFs. The dominant IMFs (5–7) were identified by the DFA algorithm and reconstructed VGA signal has been formed by the summation of IMF5–IMF7. Six entropy-based features (ApEn, SampEn, ShEn, ReEn, TsEn and PeEn) have been extracted from the reconstructed VAG signals. Individual features were given as an input to LS-SVM. For example, from Table 5, the first row signifies the classification performance of ApEn and similarly, the classification was carried out for the rest of the features. A vector of features has been formed by combining the six features

$$\text{vector} = [\text{ApEn}, \text{SampEn}, \text{ShEn}, \text{ReEn}, \text{TsEn}, \text{PeEn}]\,. \quad (15)$$

In Table 5, the vector label in the feature column represents the classification performance of a feature vector consisting six entropies (ApEn, SampEn, ShEn, ReEn, TsEn and PeEn) as elements. From Table 5, it can be seen that using SampEn as an input parameter, LS-SVM gave a sensitivity of 94.44%, which was the highest among the other features and gave an accuracy of 82.02%. The highest accuracy of 86.61% was obtained by using PeEn as a parameter. PeEn performed extremely well giving the highest accuracy of 86.61% with a sensitivity of 91.07%. MCC for PeEn was also the highest with 0.7082 and provided a low FDR rate of 0.1206. The vector of entropies (ApEn, SampEn, ShEn, ReEn, TsEn and PeEn) gave an accuracy of 84.26%, MCC of 0.6544 and FDR of 0.1355 which was quite better than other entropies.

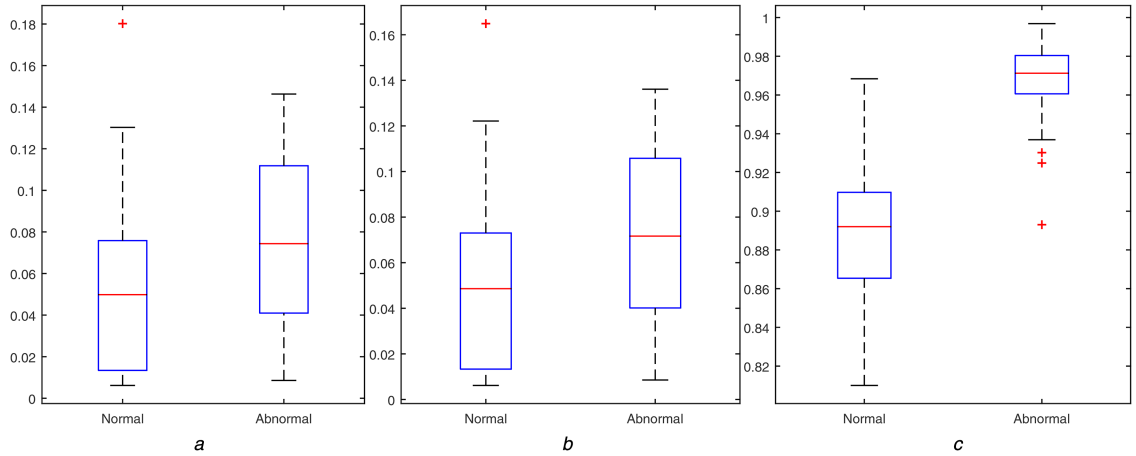

Fig. 5 *Boxplots of VAG signal of both healthy and abnormal persons*
(a) ReEn, ***(b)*** TsEn, ***(c)*** PeEn

Table 5 Classification performance of extracted features from the reconstructed VAG signal

Features	SEN	SPE	ACC	PPV	NPV	MCC	FDR	AUC
ApEn	0.8947	0.5312	0.7640	0.7727	0.7391	0.4669	0.2272	0.6600 ± 0.0592
SampEn	0.9444	0.6285	0.8202	0.7968	0.88	0.6227	0.2031	0.6465 ± 0.0598
ShEn	0.8947	0.5	0.7528	0.7611	0.7272	0.4391	0.2388	0.6486 ± 0.0597
ReEn	0.8793	0.4193	0.7191	0.7391	0.65	0.3409	0.2608	0.6620 ± 0.0591
TsEn	0.8421	0.4687	0.7078	0.7384	0.625	0.3361	0.2615	0.6610 ± 0.0580
PeEn	0.9107	0.7878	0.8661	0.879	0.8387	0.7082	0.1206	0.7250 ± 0.0556
Vector	0.8947	0.7500	0.8426	0.8647	0.8000	0.6544	0.1355	0.6816 ± 0.0582

Table 6 Classification performance of extracted features from IMFs of VAG signals

Features	SEN	SPE	ACC	PPV	NPV	MCC	FDR	AUC
ApEn	0.8947	0.5937	0.7865	0.7968	0.76	0.5215	0.2031	0.5408 ± 0.0622
SampEn	0.9107	0.7878	0.8651	0.8793	0.8387	0.7082	0.1206	0.5975 ± 0.0613
ShEn	0.8947	0.687	0.8202	0.8360	0.7857	0.6016	0.1639	0.5103 ± 0.0623
ReEn	0.8889	0.7428	0.8314	0.8421	0.8125	0.6430	0.1578	0.5160 ± 0.0623
TsEn	0.8644	0.6060	0.7717	0.7968	0.7142	0.4903	0.2031	0.5294 ± 0.0623
PeEn	0.9272	0.8529	0.8988	0.9107	0.8787	0.7848	0.0892	0.7224 ± 0.557
vector	0.9107	0.7941	0.8666	0.8793	0.8437	0.7138	0.1252	0.5867 ± 0.0616

Similarly, Table 6 gives the classification performance of features extracted from IMFs. The dominant IMFs (5–7) were identified by the DFA algorithm and entropy-based features were extracted from IMF5–IMF7. The first row of Table 6 gives the classification performance of ApEn. In this case, ApEn extracted from IMF5–IMF7 has been considered as a vector feature of ApEn, i.e.

$$\text{ApEn} = [\text{ApEn of IMF5}, \text{ApEn of IMF6}, \text{ApEn of IMF7}] \quad (16)$$

A similar classification was carried out for other features. A feature vector consisting of six entropies extracted from IMF5–IMF7 was also given as input to LS-SVM. In Table 6, the vector in the column features represents the feature vector. Hence, this feature vector consisted of 6×3 elements. The classification results have been shown in Table 6. From Table 6, a similar inference can be observed. IMFs (5–7) as a vector of PeEn gave the highest accuracy of 89.88% were obtained, MCC of 0.7848 and with low FDR of 0.089. The vector of all entropies for IMFs gave an accuracy of 86.66% with a sensitivity of 91.07%. It gave an MCC of 0.7138 with low FDR of 0.1252.

A receiver operating characteristic (ROC) curve is another effective measure of the classifier. It is a graphical representation of false positive rate (FPR, FPR = 1−specificity) versus true positive rate (TPR, also named sensitivity). The ROC-AUC curve provides how adequately a classifier technique would be able to diagnose among different classes [52, 53]. The ROC plot for reconstructed and dominant IMFs of the VAG signals is given in Fig. 6.

From Tables 5 and 6, it can be observed that PeEn gave the highest ROC curve in both cases, reconstructed VAG (0.7250 ± 0.0556) and IMFs (0.7224 ± 0.557). While vector of entropies gave ROC of 0.6816 ± 0.0582 for reconstructed VAG signals and 0.5867 ± 0.0616 for dominant IMFs. These parameters implied that the LS-SVM as a classifier precisely categorised a larger number of VAG signals between healthy and abnormal classes.

4 Discussion

The traditional signal processing techniques fail in the analysis of the non-stationary and non-linear signals since they assume that signals are linear and periodic in nature. Considering these aspects, non-linear signal processing techniques and entropy-based feature extraction techniques have been proposed. This work has focused on feature extraction methodologies and classification. In this work, the VAG signals were decomposed into IMFs using CEEMDAN. Figs. 2*a* and *b* depict the IMFs obtained from the VAG signals for healthy and abnormal subjects, respectively. The VAG signal was reconstructed by identifying the dominant IMFs (5–7) and the reconstructed VAG signal can be observed in Fig. 3.

The analysis has been carried out for all 89 VAG signals. Different entropy-based features (ApEn, SampEn, ShEn, ReEn, TsEn and PeEn) were computed for obtaining the characteristic of VAG signal. The features were extracted from reconstructed VAG signals and dominant IMFs (5–7). Tables 1–3 gave the mean and

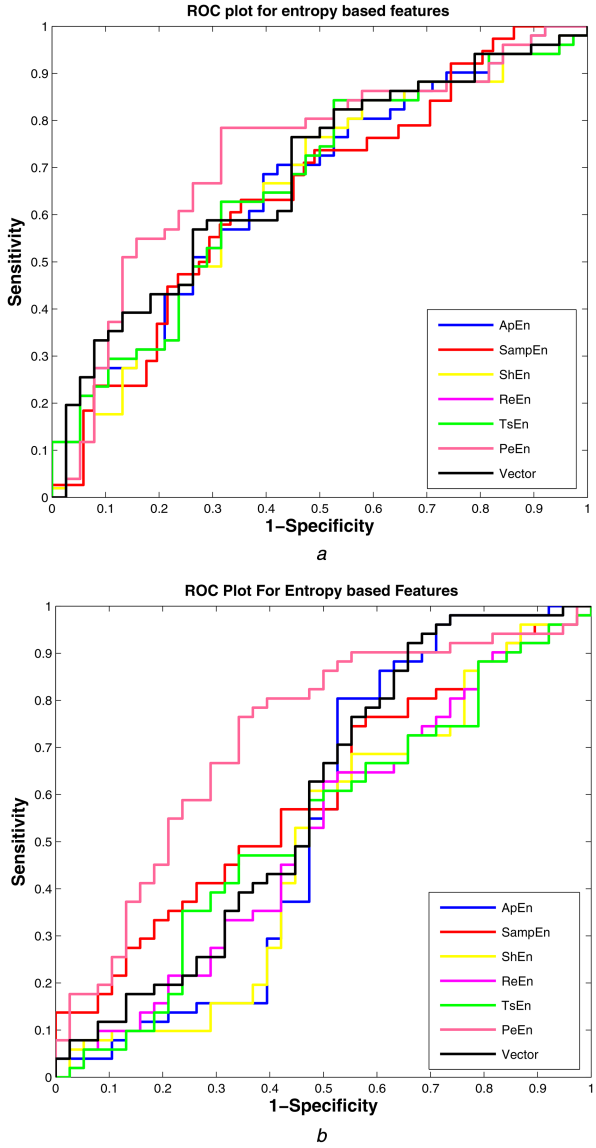

Fig. 6 *Performance of ROC of extracted features*
(a) ROC of reconstructed VAG, ***(b)*** ROC of IMFs

Table 7 Complexity of the extracted features

Features	ApEn	SampEn	ShEn
complexity	$O(N^2)$	$O(N^{3/2})$	$O(N\log(N))$

Features	ReEn	TsEn	PeEn
complexity	$O(N\log(N))$	$O(N\log(N))$	$O(N)$

Table 8 Comparison of the proposed methodology with existing non-linear studies

	EMD [19]	EEMD [23]	EEMD [24]	Our work
ACC, %	85.30	83.56	86.52	86.61
SEN	NA	0.944	0.9412	0.9107
SPE	NA	0.8	0.7632	0.7878
MCC	NA	0.6599	0.6227	0.7082
classifier	NA	SVM	random forest	LS-SVM

SD of extracted features. As observed from the table, entropies extracted from abnormal VAG signals were higher with respect to normal VAG signals. These statistical results gave a favourable way for building a classification model. The extracted features were given as input to LS-SVM.

This work compared the performance of entropy-based features. The classification was carried out with features extracted from the reconstructed VAG signal and IMFs. The classification performance has been presented in Tables 5 and 6. PeEn performed extremely well with respect to other entropies. PeEn gave the highest classification accuracy as observed in Tables 5 and 6. From Tables 5 and 6, it also inferred that the vector consisting of all entropies also provided a better classification accuracy.

Furthermore, we also compute the computational complexity of the whole system which depends on preprocessing technique, feature extraction technique and classification. In this work, the preprocessing (CEEMDAN) and classification (LS-SVM) remain same while feature extraction techniques differ with respect to different entropies. The computational complexity of the whole system would be summation of CEEMDAN, entropies and LS-SVM which is given as

$$\text{Complexity of whole system} = O(\text{CEEMDAN}) + O(\text{Entropies}) + O(\text{LS}-\text{SVM}) \quad (17)$$

The computational complexity of CEEMDAN would be the approximate equivalent to EMD/EEMD. Wang *et al.* [54] had computed the computational complexity of EMD/EEMD and it is $O(N\log N)$. Olivier stated that the computational complexity of LS-SVM depends on the sample size and no of features given as input to the classifier. The computational complexity of LS-SVM computed is $O(N_2)$ [55, 56].

Table 7 shows the computational complexity of entropy-based features. ShEn, ReEn and TsEn entropies are computed by FFT which has the computational complexity of $O(N\log(N))$. Hence the computational complexity of ShEn, ReEn and TsEn is considered as $O\log(N)$. The computational complexity of ApEn is $O(N^2)$ [35] and Pan *et al.* [40] computed the computational complexity of SampEn as $O(N^{3/2})$. PeEn provided the simple computation having the computational complexity of $O(N)$.

PeEn provided a high classification accuracy with the low computational complexity of $O(N)$. Thus, a simple, robust and low computational diagnostic system with PeEn as feature extraction technique could be designed. The computational complexity of the proposed system would be the summation of the computational complexity of CEEMDAN, PeEn, and LS-SVM. Hence, the computational complexity of the proposed system would be

$$O(N\log N) + O(N) + O(N^2) \simeq O(N^2) \quad (18)$$

We have also compared our proposed methodology with the previous studies related to non-linear signal processing studies and it has been shown in Table 8. From the table, it can be observed that our proposed method with CEEMDAN and PeEn as feature extraction technique performs better with respect to other methods. PeEn has given the highest accuracy of 86.61% with MCC of 0.7082 with respect to other non-linear studies. Chen *et al.* [19] have used HHT method for time–frequency analysis of the VAG signals. While Wu *et al.* [23] have used three entropies (symbolic entropy, ApEn, fuzzy entropy) and three distinct envelope amplitude parameters (mean, SD and root-mean-squared values) of distinct signals which gave an accuracy of 83.56% with the highest sensitivity of 0.9444. Our proposed method also performed well with respect to work of Nalband *et al.* [24] where only three entropies (TsEn, PeEn and spectral entropy) were studied.

The concluded work focused on pattern classification of VAG signals. Non-linear signal processing technique followed by entropy-based feature extraction was studied. The proposed methodology provided a better classification accuracy in distinguishing healthy and abnormal VAG signals only. The performance of various entropies was compared and their computational complexity was also considered. Furthermore, the computational complexity of the proposed system was also computed. Hence, with the idea of designing simple, non-invasive and low computational computer aided diagnostic system in a clinic of the physician could be built in future scope.

5 Conclusion

In this work, CEEMDAN, a novel technique for the analysis of VAG signals which are non-linear and non-stationary is studied. It decomposes the VAG signals into IMFs. Entropy-based features are extracted from dominant IMFs and reconstructed VAG signal. The extracted features provided distinct distinguishability between healthy and abnormal VAG classes and were given as inputs to the classifier. LS-SVM with RBF as kernel function is used as classifying technique and the performance of extracted features was evaluated. PeEn gave the highest accuracy of 86.61% for reconstructed VAG signal. The computed computational complexity of PeEn having an order of $O(N)$ provided a simple, robust and low computational feature extraction technique along with good classification accuracy. The proposed methodology which included CEEMDAN as preprocessing techniques, PeEn as feature extraction and LS-SVM, provided an effective tool for developing a computer aided diagnostics system for knee-joint disorders.

6 Acknowledgments

The authors were highly grateful to Rangaraj M. Rangayyan for providing the data set. The data acquisition for VAG signal was carried out by team led by Rangaraj M. Rangayyan, Gordon D. Bell, Cyril B. Frank, Sridhar Krishnan and Yuan-Ting Zhang of University of Calgary, Canada.

7 References

[1] Maquet, P.G.: '*Biomechanics of the knee: with application to the pathogenesis and the surgical treatment of osteoarthritis*' (Springer-Verlag, Berlin Heidelberg, 2012)

[2] Bonnin, M., Chambat, P.: '*Osteoarthritis of the Knee*' (Springer-Verlag, Paris, 2008)

[3] Krishnan, S., Rangayyan, R.M., Bell, G.D., *et al.*: 'Adaptive time-frequency analysis of knee joint vibroarthrographic signals for noninvasive screening of articular cartilage pathology', *IEEE Trans. Biomed. Eng.*, 2000, **47**, (6), pp. 773–783

[4] Rangayyan, R.M., Wu, Y.F.: 'Screening of knee-joint vibroarthrographic signals using statistical parameters and radial basis functions', *Med. Biol. Eng. Comput.*, 2008, **46**, pp. 223–232

[5] Rangayyan, R.M., Wu, Y.: 'Analysis of vibroarthrographic signals with features related to signal variability and radial-basis functions', *Ann. Biomed. Eng.*, 2009, **37**, pp. 156–163

[6] Rangayyan, R.M., Wu, Y.: 'Screening of knee-joint vibroarthrographic signals using probability density functions estimated with Parzen windows', *Biomed. Signal Proc. Control*, 2010, **5**, pp. 53–58

[7] Rangayyan, R.M., Oloumi, F., Wu, Y., *et al.*: 'Fractal analysis of knee-joint vibroarthrographic signals via power spectral analysis', *Biomed. Signal Proc. Control*, 2013, **8**, pp. 23–29

[8] Shark, L.K., Chen, H., Goodacre, J.: 'Knee acoustic emission: a potential biomarker for quantitative assessment of joint ageing and degeneration', *Med. Eng. Phys.*, 2011, **33**, (5), pp. 534–545

[9] Mascaro, B., Prior, J., Shark, L.K., *et al.*: 'Exploratory study of a non-invasive method based on acoustic emission for assessing the dynamic integrity of knee joints', *Med. Eng. Phys.*, 2009, **31**, (8), pp. 1013–1022

[10] Baczkowicz, D., Majorczyk, E.: 'Joint motion quality in vibroacoustic signal analysis for patients with patellofemoral joint disorders', *BMC Musculoskelet. Disord.*, 2014, **15**, p. 426

[11] Baczkowicz, D., Majorczyk, E., Krecisz, K.: 'Age-related impairment of quality of joint motion in vibroarthrographic signal analysis', *BioMed Res. Int.*, 2015, **2015**, http://dx.doi.org/10.1155/2015/591707

[12] Baczkowicz, D., Majorczyk, E.: 'Joint motion quality in chondromalacia progression assessed by vibroacoustic signal analysis', *PM&R*, 2016, **8**, (11) pp. 1065–1071

[13] Yang, S., Cai, S., Zheng, F., *et al.*: 'Representation of fluctuation features in pathological knee joint vibroarthrographic signals using kernel density modeling method', *Med. Eng. Phys.*, 2014, **36**, (10), pp. 1305–1311

[14] Wu, Y., Krishnan, S., Rangayyan, R.M.: 'Computer-aided diagnosis of knee-joint disorders via vibroarthrographic signal analysis: a review', *Crit. Rev. Biomed. Eng.*, 2010, **38**, pp. 201–224

[15] Wu, Y.: '*Knee joint vibroarthrographic signal processing and analysis*' (Springer-Verlag, Berlin Heidelberg, 2014)

[16] Nalband, S., Sundar, A., Prince, A.A., *et al.*: 'Feature selection and classification methodology for the detection of knee-joint disorders', *Comput. Methods Programs Biomed.*, 2016, **127**, pp. 94–104

[17] Huang, N.E., Shen, Z., Long, S.R., *et al.*: 'The empirical mode decomposition and the Hilbert spectrum for nonlinear and non-stationary time series analysis', *Proc. R. Soc. London A, Math. Phys. Eng. Sci.*, 1998, **454**, (1971), pp. 903–995

[18] Wu, Y., Cai, S., Xu, F., *et al.*: 'Chondromalacia patellae detection by analysis of intrinsic mode functions in knee joint vibration signals'. World Congress on Medical Physics and Biomedical Engineering, Beijing, China, 26–31 May 2012 (IFMBE, **39**), pp. 493–496

[19] Chen, J.C., Tung, P.C., Huang, S.F., *et al.*: 'Extraction and screening of knee joint vibroarthrographic signals using the empirical mode decomposition method', *Int. J. Innov. Comput., Inf. Control*, 2013, **9**, (6), pp. 2689–2700

[20] Mishra, V.K., Bajaj, V., Kumar, A., *et al.*: 'Analysis of als and normal emg signals based on empirical mode decomposition', *IET Sci. Meas. Technol.*, 2016, **10**, (8), pp. 963–971

[21] Wu, Z., Huang, N.E.: 'Ensemble empirical mode decomposition: a noise-assisted data analysis method', *Adv. Adapt. Data Anal.*, 2009, **01**, (01), pp. 1–41

[22] Wu, Y., Yang, S., Zheng, F., *et al.*: 'Removal of artifacts in knee joint vibroarthrographic signals using ensemble empirical mode decomposition and detrended fluctuation analysis', *Physiol. Meas.*, 2014, **35**, (3), pp. 429–439

[23] Wu, Y., Chen, P., Luo, X., *et al.*: 'Quantification of knee vibroarthrographic signal irregularity associated with patellofemoral joint cartilage pathology based on entropy and envelope amplitude measures', *Comput. Methods Programs Biomed.*, 2016, **130**, pp. 1–12

[24] Nalband, S., Sreekrishna, R.R., Prince, A.A.: 'Analysis of knee joint vibration signals using ensemble empirical mode decomposition', *Procedia Comput. Sci.*, 2016, **89**, pp. 820–827

[25] Colominas, M.A., Schlotthauer, G., Torres, M.E.: 'Improved complete ensemble EMD: a suitable tool for biomedical signal processing', *Biomed. Signal Proc. Control*, 2014, **14**, pp. 19–29

[26] Sadek, I., Biswas, J., Fook, V.F.S., *et al.*: 'Automatic heart rate detection from FBG sensors using sensor fusion and enhanced empirical mode decomposition'. 2015 IEEE Int. Symp. Signal Processing and Information Technology (ISSPIT), 2015, pp. 349–353

[27] Lahmiri, S., Boukadoum, M.: 'An application of the empirical mode decomposition to brain magnetic resonance images classification'. 2013 IEEE Fourth Latin American Symp. Circuits and Systems (LASCAS), 2013, pp. 1–4

[28] Lahmiri, S., Boukadoum, M.: 'Automated detection of circinate exudates in retina digital images using empirical mode decomposition and the entropy and uniformity of the intrinsic mode functions', *Biomed. Eng./Biomed. Tech.*, 2014, **59**, (4), pp. 357–366

[29] Cirugeda, E., Cuesta, D., Miró, P., *et al.*: 'A new algorithm for quadratic sample entropy optimization for very short biomedical signals: application to blood pressure records', *Comput. Methods Programs Biomed.*, 2014, **114**, (3), pp. 231–239

[30] Acharya, U.R., Faust, O., Sree, V., *et al.*: 'Linear and nonlinear analysis of normal and CAD-affected heart rate signals', *Comput. Methods Programs Biomed.*, 2014, **113**, (1), pp. 55–68

[31] Kannathal, N., Choo, M.L., Acharya, U.R., *et al.*: 'Entropies for detection of epilepsy in EEG', *Comput. Methods Programs Biomed.*, 2005, **80**, (3), pp. 187–194

[32] Sharma, R., Pachori, R.B., Rajendra Acharya, U.: 'An integrated index for the identification of focal electroencephalogram signals using discrete wavelet transform and entropy measures', *Entropy*, 2015, **17**, (8), pp. 5218–5240

[33] Pincus, S.: 'Approximate entropy as a measure of system complexity', *Proc. Natl. Acad. Sci.*, 1991, **88**, (6), pp. 2297–2301

[34] Pincus, S.M., Viscarello, R.R.: 'Approximate entropy: a regularity measure for fetal heart rate analysis', *Obstet. Gynecol.*, 1992, **79**, pp. 249–255

[35] Manis, G.: 'Fast computation of approximate entropy', *Comput. Methods Programs Biomed.*, 2008, **91**, (1), pp. 48–54

[36] Richman, J.S., Moorman, J.R.: 'Physiological time series analysis using approximate entropy and sample entropy', *Am. J. Physiol. Heart Circ. Physiol.*, 2000, **278**, pp. H2039–H2049

[37] Burioka, N., Miyata, M., Cornélissen, G., *et al.*: 'Approximate entropy in the electroencephalogram during wake and sleep', *Clin. EEG Neurosci.*, 2005, **36**, pp. 21–24

[38] Song, Y., Crowcroft, J., Zhang, J.: 'Automatic epileptic seizure detection in EEGs based on optimized sample entropy and extreme learning machine', *J. Neurosci. Methods*, 2012, **210**, pp. 132–146

[39] Yentes, J.M., Hunt, N., Schmid, K.K., *et al.*: 'The appropriate use of approximate entropy and sample entropy with short data sets', *Ann. Biomed. Eng.*, 2013, **41**, (2), pp. 349–365

[40] Pan, Y.H., Wang, Y.H., Liang, S.F., *et al.*: 'Fast computation of sample entropy and approximate entropy in biomedicine', *Comput. Methods Programs Biomed.*, 2011, **104**, (3), pp. 382–396

[41] Shannon, C.E.: 'A mathematical theory of communication', *Bell Syst. Tech. J.*, 1948, **27**, (July 1928), pp. 379–423

[42] Rényi, A.: 'On measures of entropy and information', *Entropy*, 1961, **547**, (c), pp. 547–561

[43] Robert, S.: 'The Tsallis entropy of natural information', *Physica A, Stat. Mech. Appl.*, 2007, **386**, (1), pp. 101–118

[44] Bandt, C., Pompe, B.: 'Permutation entropy: a natural complexity measure for time series', *Phys. Rev. Lett.*, 2002, **88**, (17), p. 174102

[45] Zanin, M., Zunino, L., Rosso, O.A., *et al.*: 'Permutation entropy and its main biomedical and econophysics applications: a review', *Entropy*, 2012, **14**, (8), pp. 1553–1577

[46] Kalpakis, K., Yang, S., Hu, P.F., *et al.*: 'Permutation entropy analysis of vital signs data for outcome prediction of patients with severe traumatic brain injury', *Comput. Biol. Med.*, 2015, **56**, pp. 167–174

[47] Vapnik, V.N., Chervonenkis, A.Y.: 'On the uniform convergence of relative frequencies of events to their probabilities' *Theory Probab. Appl.*, 1971, **16**, (2), pp. 264–280

[48] Vapnik, V.N.: '*The nature of statistical learning theory*', vol. **8** (IEEE Transactions on Neural Networks, Wiley, New York, 1995)

[49] Cai, S., Wu, Y., Xiang, N., *et al.*: 'Detrending knee joint vibration signals with a cascade moving average filter'. Proc. of the Annual Int. Conf. of the IEEE Engineering in Medicine and Biology Society, EMBS, 2012, pp. 4357–4360

[50] De Brabanter, K., Karsmakers, P., Ojeda, F.*, et al.*: '*LS-SVMlab toolbox user's guide: version 1.7*' (Katholieke Universiteit Leuven, Leuven-Heverlee, Belgium, 2010)
[51] Kohavi, R.: 'A study of cross-validation and bootstrap for accuracy estimation and model selection'. Int. Joint Conf. Artificial Intelligence, 1995, vol. 14, pp. 1137–1143
[52] Zweig, M.H., Campbell, G.: 'Receiver-operating characteristic (ROC) plots: a fundamental evaluation tool in clinical medicine [published erratum appears in Clin Chem 1993 Aug;39(8):1589]', *Clin. Chem.*, 1993, **39**, pp. 561–577
[53] Greiner, M., Pfeiffer, D., Smith, R.D.: 'Principles and practical application of the receiver-operating characteristic analysis for diagnostic tests', *Prev. Vet. Med.*, 2000, **45**, pp. 23–41
[54] Wang, Y.H., Yeh, C.H., Young, H.W.V.*, et al.*: 'On the computational complexity of the empirical mode decomposition algorithm', *Physica A, Stat. Mech. Appl.*, 2014, **400**, pp. 159–167
[55] Chapelle, O.: 'Training a support vector machine in the primal', *Neural Comput.*, 2007, **19**, (5), pp. 1155–1178
[56] Bottou, L., Chih, J.L.: 'Support vector machine solvers', '*Large scale kernel machines*' 2007, **3**, (1), pp. 301–320